Radiation Dose and Risk from Fluoroscopically Guided Percutaneous Transhepatic Biliary Procedures

John Stratakis, MSc, John Damilakis, PhD, Adam Hatzidakis, MD, Kostas Perisinakis, PhD, and Nicholas Gourtsoyiannis, MD

PURPOSE: To estimate radiation dose and associated risks after fluoroscopically guided percutaneous transhepatic biliary (PTB) drainage and stent implantation procedures.

MATERIALS AND METHODS: Organ and effective doses, normalized to dose–area product (DAP), were estimated for PTB procedures with use of a Monte Carlo transport code and an adult mathematical phantom. Exposure parameters from 51 consecutive patients were used to determine average examination parameters for biliary drainage and stent implantation procedures. Thermoluminescent dosimeters were used in an anthropomorphic phantom to verify Monte Carlo calculations. Radiation-induced cancer and genetic risks were estimated.

RESULTS: The results consist of doses normalized to DAP so patient dose from any technique and x-ray unit can be easily calculated for left and right biliary access and for separate or combined biliary and metallic stent implantation sessions. A good agreement was found between Monte Carlo–calculated data and data derived from thermoluminescent dosimetry. The average effective dose varied from 1.8 to 5.4 mSv depending on procedure approach (left vs right access) and procedure scheme. A maximum effective dose of 13 mSv was estimated for 30 minutes of fluoroscopy.

CONCLUSIONS: Doses delivered to patients undergoing PTB procedures are comparable to those that arise from computed tomography protocols. Radiation-induced cancer risk may be considerable for young patients undergoing PTB drainage and stent implantation procedures.

J Vasc Interv Radiol 2006; 17:77–84

Abbreviations: DAP = dose–area product, LAO = left posterior oblique, MCNP = Monte Carlo N-particle, PA = posteroanterior, PTB = percutaneous transhepatic biliary, RAO = right posterior oblique, TLD = thermoluminescent dosimetry

PERCUTANEOUS transhepatic biliary (PTB) procedures are commonly performed in the interventional radiology laboratory under fluoroscopic guidance (1). PTB drainage and stent implantation are commonly indicated in patients with biliary duct obstruction caused by unresectable primary or metastatic malignancies (2,3). Prolonged fluoroscopy times in PTB procedures are frequently observed, depending on the grade of difficulty and the cooperation of the patient. Additional time is occasionally needed for simultaneous metallic stent placements.

There is significant concern related to radiation exposure of patients undergoing fluoroscopically guided interventional procedures (4,5). National and regional authorized bodies point out the increasing number of interventional radiologic procedures (6) and recommend the use of patient dose surveys and the establishment of dose reference levels to optimize radiation dose (7–9). When beam characteristics and procedure geometry change throughout the procedure, an accurate assessment of patient dose and risk can be cumbersome (10). Patient size and clinical condition may also affect examination technique and consequently the dose to the patient.

Several methods have been used to determine doses delivered to patients during interventional radiologic procedures. Organ and effective dose data may be measured with use of anthropomorphic phantoms loaded with thermoluminescent dosimetry (TLD) crystals located at specific anatomic locations (11). Surface doses can be acquired from x-ray tube output data (12–14). Effective dose can be estimated from measured dose–area product (DAP) data or derived from energy imparted to the patient (15,16). Monte Carlo techniques and mathe-

From the Department of Medical Physics, Faculty of Medicine, University of Crete, P.O. Box 1393, 71409 Iraklion, Crete, Greece. Received May 10, 2005; accepted September 18. **Address correspondence to** J.D.; E-mail: damilaki@med.uoc.gr

None of the authors have identified a conflict of interest.

DOI: 10.1097/01.RVI.0000188754.97465.13

matical phantoms have also been employed to simulate radiation transport and estimate energy deposition in the human body (17,18). An advantage of Monte Carlo methods is that x-ray projections, patient size, and x-ray spectra are freely adjustable.

To our knowledge, there are no normalized patient dose data in the literature associated with PTB procedures. Normalized dosimetric data incorporate a major advantage in comparison with surface or air kerma measurements. Because normalized values are derived by dividing surface or air kerma reading by entrance dose or DAP rate of each exposure, they comprise data independent of exposure parameters. Operators who use DAP-normalized dosimetric data, which are technique- and instrumentation-independent values, will be able to calculate effective dose and radiation-induced detriment by multiplying total DAP of the procedure with a single conversion coefficient.

The aims of the current study were to (i) estimate radiation dose and risks related to typical PTB procedures and (ii) provide normalized-to-DAP organ and effective dose data associated with PTB procedures.

MATERIALS AND METHODS

The x-ray imaging system used in this study was a floor-mounted Siemens Axiom Artis FA angiographic unit (Siemens, Erlangen, Germany) with a digital fluorography C-arm assembly. The system was preconfigured from the manufacturer for various interventional and digital subtraction angiography procedures. A high-output, liquid-cooled x-ray tube with a triple focus of 0.3 mm, 0.6 mm, and 1.0 mm; a 12° anode angle; and an inherent filtration of 2.5 mm Al/80 kV was used. The tube housing occupied a collimation system and semitransparent wedge filters, which could be moved or rotated independently. The total filtration of the unit was estimated to be 5.5 mm Al. The x-ray tube was monitored by an ionization chamber incorporated in the collimation system for measuring the radiation dose in terms of cGy/cm^2. Total DAP for each interventional radiologic procedure and separate DAP contributions corresponding to fluoroscopy and radiography were recorded. An image intensifier of a maximum circular field size of 38 cm was used. Tube potential and current were altered through automatic exposure control.

In the current study, 51 consecutive patients with bile duct occlusion or stenosis were treated in our interventional radiology laboratory. This study was carried out in accordance with the Declaration of Helsinki and written consent was obtained from all patients. Patients were separated into three groups: group A consisted of 19 patients in whom only biliary drainage was undertaken; group B consisted of 11 patients treated with draining and metallic stent implantation in one session; and group C comprised 21 subjects treated with draining and metallic stent implantation in two different fluoroscopy courses. Age, height, and weight of every patient undergoing a PTB procedure were registered. Fluoroscopy was performed with variable tube current and voltage according to the examination protocol supplied by the manufacturer of the angiographic unit. Pulsed fluoroscopy of 15 pulses per second was used with a pulse width of 25 msec. Patient data were used to determine average examination parameters for biliary drainage and stent placement procedures. Consequently, technical and physical parameters for fluoroscopy and radiography were recorded, such as field size, fluoroscopy time, and number of radiographic exposures. In addition, DAP measurements for fluoroscopy and digital radiography were performed with use of the integrated DAP meter of the fluoroscopy system.

The fluoroscopic projections typically used in PTB procedures are: (i) the posteroanterior (PA) projection, (ii) the 25° right posterior oblique (RAO) for left access and (iii) the 25° left posterior oblique (LAO) for right access to the bile ducts. During PTB, the patient was studied in the supine position, and a puncture site was selected under fluoroscopic conditions. If a duct was not found, subsequent passages were required, which is often seen in patients with nondilated bile ducts. Subsequently, when dilation was complete, a catheter was introduced into the bile duct for external drainage or internal drainage through the duodenum. If necessary, an internal stent was used in patients with biliary obstruction.

To simulate dose distribution in the human body during a PTB procedure, the Monte Carlo N-particle code system (MCNP; version 4C2; Los Alamos National Laboratory, Los Alamos, NM) was employed (19). MCNP implements conventional mathematical figures such as planes, spheres, cylinders, and their intersections to define the geometry of a diagnostic interventional procedure. To assess radiation transport, particles' interactions were monitored from their origin to their termination. An input file supplied by the user, which contains materials composition, x-ray source specifications, and type of detectors (ie, tallies), was subsequently read by MCNP. Human anatomy was replicated by means of a hermaphroditic mathematical phantom that was constructed with use of BodyBuilder (White Rock Science, Los Alamos, NM), a commercially available package. Patient size and organs in the mathematical phantom incorporated in BodyBuilder software were freely adjustable. The mathematical phantom created represented an adult human body 1.74 m in height and 71.1 kg in weight. Composition of the human body was modeled by assigning skeletal, soft, or lung material to corresponding tissues. Internal organs have been considered homogenous in composition and density. Diagnostic energy spectra developed by Nowotny and Hofer (20) were used in the MCNP input file. Beam angle and x-ray source position were also taken into consideration within the MCNP input file, whereas field sizes were measured on the surface of the image intensifier. Carefilter (Siemens) was simulated by adding 0.3 mm of copper in the useful beam.

Organ doses were calculated for an adult mathematical phantom simulating a patient undergoing biliary drainage. Energy deposition was recorded for PA, LAO 25°, and RAO 25° projections for sessions incorporating biliary drainage only, biliary drainage and metallic stent placement in one session, or drainage and stent placement in two sessions. In each simulation, entrance surface dose was obtained with use of an f5 tally just above the surface of the phantom. Energy deposition in each of the 27 modeled organ

Table 1
Demographic Data of the Three Study Groups

	Group A (n = 19)		Group B (n = 11)		Group C (n = 21)	
Sex (M:F)	11:8		5:6		15:6	
Age Range (y)	34–89		38–71		41–74	
	Median	Mean ± SD	Median	Mean ± SD	Median	Mean ± SD
Age (y)	69	66.95 ± 10.24	67.5	64.75 ± 12.10	58	57.85 ± 11.47
Height (m)	1.65	1.66 ± 0.07	1.65	1.64 ± 0.05	1.65	1.62 ± 0.06
Weight (kg)	65	71.3 ± 12.3	63	63.8 ± 3.5	70	72 ± 8.2
BMI (kg/m^2)		25.9 ± 3.4		23.7 ± 3.4		27.4 ± 4.1

Note.—BMI = body mass index.

structures was measured with use of an f6 tally scoring the entire organ volume. The f5 and f6 tallies are mathematical detectors commonly used in Monte Carlo simulations. Organ doses were divided with total DAP to provide DAP-to-organ dose conversion factors for every projection. Calculations were performed for a 70-kV peak tube potential and for a 2.5-mm Al/0.3-mm Cu total beam filtration. Effective dose calculations normalized to DAP were performed according to the International Commission on Radiation Protection's formula in Publication 60 (21):

$$\varepsilon_{dap} = \sum_{organ_i} w_{organ_i} D_{organ_i} \qquad (1)$$

where w_{organ_i} is each tissue/organ's weighting factor introduced in International Commission on Radiation Protection Publication 60. All remainder tissues were taken into consideration when calculating effective dose. Normalized dose to the residual tissues was considered as the dose to the muscle. Moreover, dose to the bone surface was taken to be the dose to the skeleton, that is, the sum of normalized doses for cells incorporating bone density in the phantom. Dose to red bone marrow was estimated from the dose to the skeletal tissue, taking into consideration the amount of active marrow in each irradiated bone (22,23). Each imaging run simulated the deposition of approximately 5 million photons originating from the x-ray source. At that stage, the detectors had converged to a relative error of less than 1%. Simulations were performed on Pentium IV (Intel, Santa Clara, CA)–based personal computers. Each simulation consumed approximately 20 minutes of computer time. Energy deposition was calculated for the PA, RAO, and LAO projections altered by ±10° along the sagittal plane of the patient to investigate the effect of the orientation of the studied projections on the effective dose.

To verify Monte Carlo results, organ dose measurements were acquired with use of TLD and an anthropomorphic phantom (Rando; Alderson, Stanford, CA), which is cut into 36 transverse 2.5-cm-thick sections. Each slice contains a matrix of cylindrical holes for the location of TLD material. It is widely used to simulate the torso of an adult subject 1.73 m in height and 74 kg in weight. Lithium (TLD-100) and calcium fluoride (TLD-200) chips (Bicron/Harshaw; Solon, OH) were used to determine the dose to radiation-sensitive tissues at different points in the Rando phantom. TLD-200 chips were considered preferable to TLD-100 material for dose measurements at sites out of the primary beam because of their greater sensitivity. TLD crystals were calibrated with use of the same fluoroscopy system and beam quality that were used to perform the PTB procedures. The phantom was appropriately loaded with 85 TLDs at positions corresponding to the radiation-sensitive organ and tissues defined by the recommendations Publication 60 of the International Commission on Radiation Protection (21). The phantom was exposed to separate fluoroscopy courses, so as PA, LAO 25°, and RAO 25° were simulated according to the actual PTB procedure applied for patient groups A, B, and C. The same C-arm fluoroscopy system involved in the patient study was used. For each projection, the phantom was exposed to 5,000 cGy/cm^2 of radiation to reduce statistical errors in TLD signal measurements. TLDs were read immediately after each session of irradiation. Entrance skin dose was monitored by TLD-100 crystals attached on the posterior side of the phantom. DAP-normalized dose to each organ or tissue in each slice of the Rando phantom was determined from the value of all TLDs according to the equation:

$$D_{organ_i} = \frac{\sum_j f_{organ_j} d_{organ_{ij}}}{DAP} \qquad (2)$$

where f_{organ_j} is the fraction of $organ_{ij}$ contained in Rando slice j and $d_{organ_{ij}}$ is the dose to the fraction of $organ_i$ contained in phantom slice j, obtained from Perisinakis et al (24). Normalized-to-DAP patient effective dose along each projection was subsequently calculated according to equation 1.

For the purpose of this study, the peak skin dose from a typical procedure was compared to 2 Gy and 3 Gy, which are the thresholds for skin erythema and epilation, respectively (5). Stochastic risks of carcinogenesis were quantified by multiplying calculated effective dose with the risk of cancer death attributable to uniform, whole-body, low linear energy transfer irradiation for the US population (25). For the male population aged 30–39 years, 40–49 years, 50–59 years, 60–69 years, 70–79 years, and 80 years and older, the Biological Effects of Ionizing Radi-

Table 2
Operating Parameters of Radiation Exposure Recorded for Projections Involved in PTB Procedure

Imaging Parameter	PA	LAO	RAO
Fluoroscopy			
kV	73.5 ± 5.3	71.5 ± 6.1	74 ± 5
mA	29.2 ± 10.2	33.2 ± 8.6	29.9 ± 9.4
SSD (cm)	68 ± 2	70 ± 2	70 ± 2
Digital radiography			
kV	73.6 ± 8.8	74.8 ± 6	75 ± 5.6
mA	49 ± 4	59 ± 6	60 ± 6.7
No. of radiographs	4.2 ± 3	3.1 ± 2	4.7 ± 4
Contribution (%)	64.5 ± 33.2	50.7 ± 31.72	72 ± 11.2

Note.—SSD = source to skin distance.

Table 3
Average and Maximum Observed Values of Radiation Exposure Parameters Observed for Patients in Study Groups A, B, and C Involved in PTB Procedures

Parameter	Value
Fluoroscopic time (min)	11.52 ± 6.5
DAP of fluoroscopy(cGy/cm^2)	1,947 ± 1,676
DAP of digital radiography (cGy/cm^2)	405 ± 139
Total DAP (cGy/cm^2)	2,553 ± 1,997
Maximum fluoroscopy time observed	28:19
Maximum total DAP observed (cGy/cm^2)	6,071.7

Note.—Values presented as means ± SD where applicable.

ation V Committee has assigned values of 5.66, 6, 6.16, 4.81, 2.58, and 1.10 per 10^{-2} Gy as the fatal cancer risk factor. The factors for the corresponding female patient groups are 5.57, 5.41, 5.05, 3.86, and 2.27 per 10^{-2} Gy, respectively. The risk for severe hereditary effects was calculated by multiplying the dose to the gonad area by a factor of 10^{-2} Gy^{-1} (21).

Data statistical analysis was performed with use of the MedCalc statistical package (MedCalc, Mariakerke, Belgium). Results are expressed as mean values ± SD. An analysis of variance was used to investigate whether statistically significant differences existed among data of the three study groups. Moreover, a Kolmogorov-Smirnoff test confirmed that patient data (**Table 1**) followed a normal distribution. A P value $<.05$ was required for the test result to be considered significant.

RESULTS

Fifty-one consecutive patients with bile duct obstruction were treated in our institution. Demographic data for study groups A, B, and C are presented in **Table 1**. There were no statistically significant differences among the three study groups.

In **Table 2**, an overview of the technical parameters for fluoroscopy and digital radiography is given, which is derived from groups A, B, and C treated with biliary drainage and/or stent placement in our institution. Fluoroscopic time, number of radiographs, and percentage of exposure time associated with PA and lateral projections are also presented. The mean total fluoroscopy time and mean total DAP values were 11.52 minutes and 1,947 cGy/cm^2, respectively. In **Table 3**, average and maximum observed dosimetric values associated with PTB procedures are presented.

Total DAP–to–organ dose conversion coefficients derived from Monte Carlo calculations for PA, LAO 25°, and RAO 25° projections are presented in **Table 4** for all modeled organs. Tissues that received considerable amounts of radiation during a PTB procedure are the skin surface at the beam entrance area, the liver, the adrenal glands, the kidneys, and the intestine. The peak skin dose delivered to a patient undergoing a typical PTB procedure is also shown in **Table 4**. **Table 5** presents effective dose data involved in typical biliary drainage and stent implantation procedures performed in our institution, corresponding to study groups A, B, and C. Typical left-access PTB procedures involved PA and RAO projections, which required 20% and 80% of total fluoroscopic time, respectively. A right-access PTB procedure involved a combination of LAO and PA projections, which required 80% and 20% of procedure fluoroscopic time, respectively. **Figure 1** illustrates differences between Monte Carlo–calculated normalized effective doses derived and normalized data obtained from direct TLD measurements. Maximum differences did not exceed 13%. Alterations in the orientation of the fluoroscopic x-ray beam by ±10° produced no more than 7% differences in the Monte Carlo–calculated conversion coefficients.

In **Figure 2**, the dependence of radiation-induced cancer risk on the age and sex of the patient undergoing PTB procedures is illustrated. Age- and sex-averaged risk values for genetic effects resulting from PTB procedures are shown in **Table 6**.

DISCUSSION

Interventional radiologic procedures are frequently characterized by extended fluoroscopy times and a significant number of acquired images (4,5). Awareness of accurate effective and organ dose data from specific interventional radiologic procedures will help health care providers to optimize procedures so radiation dose delivered to patients is balanced with good clinical practice.

The present study was motivated by the limited dosimetric data for PTB procedures in the literature. To our knowledge, normalized effective and organ dose levels have not been reported in the literature. In addition, dosimetric data and associated risks for separate sessions of drainage and metallic stent implantation or combined procedures (ie, drainage and stent implantation) have not been reported. Entrance skin dose estimates

Table 4
Organ and Effective Dose Values Normalized over Total DAP for Projections Involved in PTB Procedures

Tissue	PA	LAO 25°	RAO 25°
Ovaries (female)*	0.61	0.51	0.555
Testes (male)*	0.01	0.01	0.01
Active bone marrow*	2.23	2.28	2.16
Lungs*	1.71	1.46	2.12
Colon*	0.18	0.21	0.28
Kidneys	14.8	17.3	15.8
Adrenal glands	14.5	16.27	14.3
Stomach*	1.02	1.09	1.52
Urinary bladder*	0.11	0.10	0.10
Gall bladder	5.76	3.89	6.090
Spleen	0.73	1.41	1.05
Pancreas	3.73	4.71	4.18
Thymus	0.18	0.13	0.23
Breasts*	0.19	0.15	0.24
Liver*	8.94	6.13	11.2
Esophagus*	0.71	0.77	0.85
Thyroid*	0.01	0.01	0.03
Heart	0.96	0.96	1.35
Skeleton*	3.11	3.16	3.10
Skin*	1.26	1.34	1.49
Skin (beam entrance)	20.5	20.7	21.7
Remainder (muscle)	1.40	1.38	1.539
Effective dose (female)	1.96	1.81	2.22
Effective dose (male)	1.84	1.70	2.11

* Organs for which the International Commission on Radiological Protection has assigned a weighting factor for the calculation of effective dose.
Note.—Values presented as μSv/cGy/cm^2.

derived from DAP measurements and patient radiation doses have been presented in two studies for a PA projection only. Cruces et al (26) have reported an effective dose of 1.1 mSv per minute of fluoroscopy and a 1,500-cGy/cm^2 mean total DAP for biliary drainage. McParland (15) has reported a mean fluoroscopy time of 7.1 minutes, a median fluoroscopy time of 4.1 minutes, a total DAP of 4,300 cGy/cm^2, and a median DAP of 2,790 cGy/cm^2 for a biliary stent insertion/removal procedure, resulting in an effective dose of 6.9 mSv with a median value of 4.5 mSv per procedure. To calculate effective dose delivered to the patients, these studies have used conversion coefficients derived from Monte Carlo calculations listed in National Radiological Protection Board report R-262 (27). However, radiographic projections used in the National Radiological Protection Board reports are rough approximations of actual projections employed in PTB procedures in terms of field size, shape, and position, and do not cover sufficiently all PTB-employed projections. Therefore, application of the National Radiological Protection Board's kidney PA or abdomen PA projections (27) may overestimate or underestimate radiation deposition on specific tissues, affecting overall estimation of effective dose. In the current study, an exact representation of the actual x-ray geometry was replicated for a variety of PTB approaches. We decided to normalize dose data to DAP because DAP changes considerably when field size changes during the procedure. DAP-normalized dose data may be useful information for other institutions to use to estimate patient doses and radiation risks. In addition, because dose reference levels for fluoroscopically guided procedures are usually expressed in terms of DAP, dosimetric data presented in this study may help health care providers to establish, apply, and optimize dose reference levels in their institutions.

According to the findings of our study, organs that receive considerable amounts of radiation are the liver, adrenal glands, kidneys, intestine, and gallbladder. Comparison of Monte Carlo–calculated organ doses with values obtained from direct phantom measurements present differences lower than 20%. Individual organ dose differences may be attributed to divergence in the location and volume of organs in the Rando phantom and organs in the BodyBuilder phantom adopted for our Monte Carlo simulations. Errors introduced by TLD are expected to be approximately 15% (24). Despite of the differences in individual organ dose values, comparison of Monte Carlo–calculated effective dose data show very good agreement with effective dose derived from TLD measurements (**Fig 1**).

According to the findings of the current study, the average effective dose from a typical PTB procedure varied from 1.8 mSv to 5.4 mSv depending on procedure approach (left or right access), application scheme (one- or two-step procedure) and sex of the patient. Mean total fluoroscopy time and mean total DAP values of 11.52 minutes and 1,947 cGy/cm^2, respectively, correspond to an average effective dose of 3.2 mSv for a patient undergoing a single drainage procedure, which usually involves a PA projection only. Consequently, considerable differences are observed in dosimetric data reported in this study compared with data reported by other investigators (14,15,26). Lower effective doses reported in this study may be partly attributed to the fact that a low-dose pulsed fluoroscopy system was employed in our institution. Effective dose differences as great as 12% occurred for left or right transhepatic access in percutaneous drainage or metallic stent placement. Biliary interventions with a right access produce greater effective doses because a lateral projection is almost exclusively used throughout a right-access PTB procedure. Accordingly, higher tube voltage and current are required to penetrate through the patient. In addition, the radiation field is distributed over more organs through a lateral projection. Female patients are subjected to slightly greater doses than male patients. An average difference of 6% was observed between effective doses delivered to female and male patients. This difference in effective dose was to be expected, as female gonads received higher doses than male gonads in all cases.

Table 5
Effective Dose Values for Typical PTB Procedures*

	PTB Drainage Only (1,000 cGy/cm^2)		One-step PTB Drainage and Stent Placement (2,500 cGy/cm^2)		PTB Stent Placement Only (1,500 cGy/cm^2)†	
Effective Dose	Right Access	Left Access	Right Access	Left Access	Right Access	Left Access
In female patients (mSv)	2.167	1.928	5.420	4.820	3.250	2.892
In male patients (mSv)	2.057	1.815	5.143	4.540	3.086	2.723

* Right access PTB, 80%/20% for PA/LAO; left access PTB, 20%/80% for PA/RAO.
† PTB stent placement procedure after a singe drainage procedure (two-step procedure).

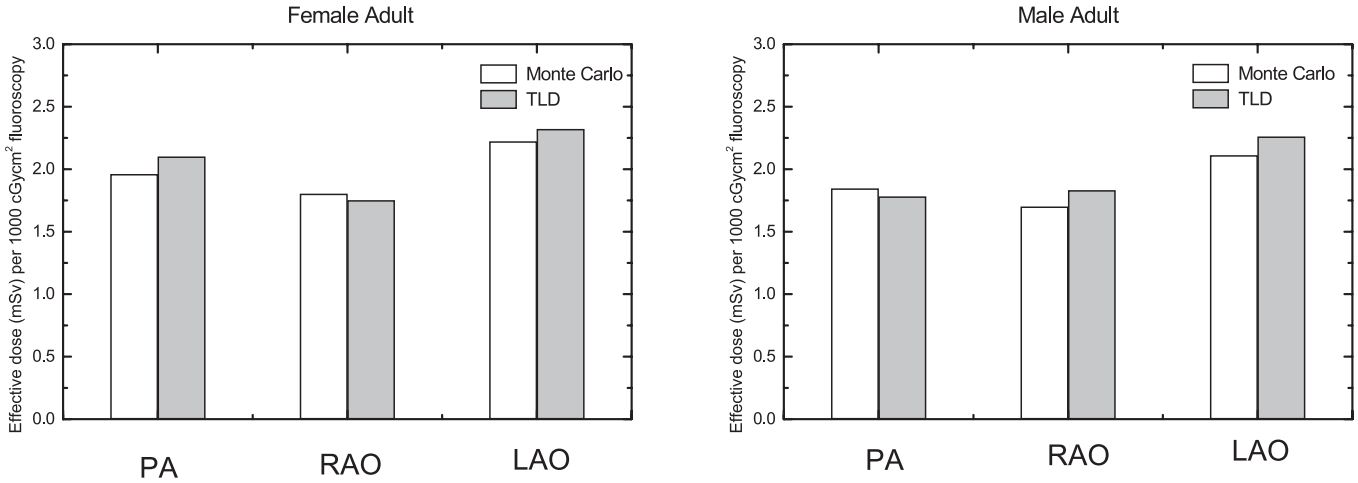

Figure 1. Comparison of effective doses derived from Monte Carlo calculations and effective doses measured by TLD crystals for male and female patients undergoing PTB procedures. A DAP value of 1,000 cGy/cm^2 was used for PA, LAO, and RAO projections.

Organ and effective dose values produced in this study may be considered comparable to those arising from computed tomography (CT) examinations of the trunk (28). The maximum fluoroscopy time and DAP exposure observed in our institution were 28.3 minutes and 6,072 cGy/cm^2, respectively, which correspond to an effective dose of 13 mSv. Patients treated with PTB procedures may endure even higher radiation doses as a result of extended exposure times affected by the clinical condition of the patient. Apparently, puncture location and lack of dilation of the biliary ducts may prolong the procedure (29).

Maximum estimated peak skin dose delivered to a patient undergoing a PTB procedure enduring approximately 30 minutes of fluoroscopy and 6,000 cGy/cm^2 was 15 times lower than the 2-Gy threshold for deterministic effects. The radiogenic stochastic risk associated with PTB procedures may be tolerable when compared with the nominal risk for fatal cancer induction and detrimental hereditary disorders (**Table 6**). Radiation-induced cancer risks with respect to age and sex of individuals undergoing PTB procedures are illustrated in **Figure 2**. Compared with male individuals of the same age, young female patients (30–39 years) are subjected to increased risk. Moreover, the risk for older female subjects is lower than the corresponding risk for male patients. In general, younger individuals are subject to considerably higher risk than older patients. Consequently, even though biliary procedures are more likely to be performed in older patients, care must be taken when these procedures involve young individuals.

Minimization of patient exposure during fluoroscopically guided procedures is a requirement of good clinical practice. Awareness of radiation dose and associated risks will help reduce doses delivered to patients and medical personnel. Pulsed instead of continuous fluoroscopy on units with high total filtration may produce substantial dose reductions. Variations in examination technique and equipment may also significantly affect fluoroscopy times. Moreover, periodic quality assurance of the fluoroscopy equipment should be performed to ensure image quality and radiation safety.

CONCLUSION

In conclusion, radiation doses and risks are presented for a variety of PTB approaches. Normalized dose data presented in this study will enable patient dose estimation at other institutions. Doses from PTB procedures were considered comparable to those arising from CT procedures. Radiation risk to patients should not be disregarded, especially for younger patients, as interventional radiologic procedures often involve prolonged fluoroscopy times and patients may

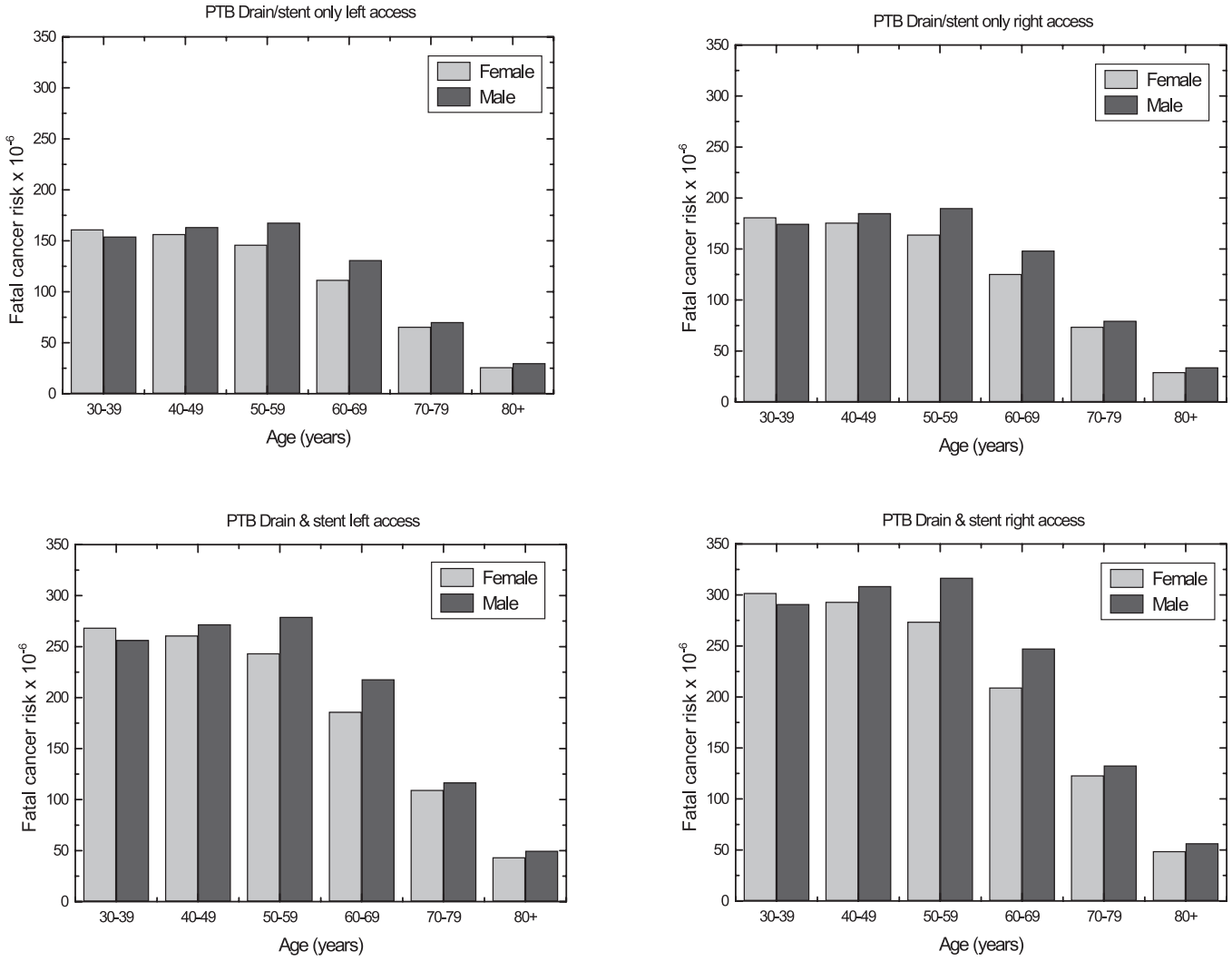

Figure 2. Illustration of the dependence of radiation-induced cancer risk on the age and sex of an individual undergoing fluoroscopically guided PTB procedures. Risk estimations are shown for single procedures involving biliary drainage or metallic stent placement and combined interventional procedures involving drainage and stent placement in one session.

Table 6 Risks for Genetic Defects after Typical PTB Procedures

Procedure*	Access	Genetic Defect Risk per Million: Female	Genetic Defect Risk per Million: Male
PTB drainage only	Left	6	0.7
	Right	5.5	0.5
PTB stent placement only	Left	8.2	1
	Right	6	0.8
PTB drainage and stent placement	Left	15	1.8
	Right	29	1.3

* PA and LAO/RAO fluoroscopy resulting in 1,000 cGy/cm^2 (PTB drain only), 2,500 cGy/cm^2 (PTB drain and stent placement), and 1,500 cGy/cm^2 (PTB stent placement only).

undergo more than one interventional radiologic procedure. In all cases, efforts should be made to limit radiation burden by optimization of fluoroscopic approaches through procedure and equipment quality control.

References

1. Lammer J, Neumayer K. Biliary drainage endoprostheses: experience with 201 placements. Radiology 1986; 159:625–629.
2. Cotton PB. Management of malignant bile duct obstruction. J Gastroenterol Hepatol 1990; 5(suppl 1):63–67.
3. Born P, Rösch T, Bruhl K, et al. Long term outcome in patients with advanced hilar bile duct tumors undergoing palliative endoscopic or percutaneous drainage. Z Gastroenterol 2000; 38: 483–489.
4. Food and Drug Administration. Public Health Advisory: avoidance of serious x-ray induced skin injuries to patients during fluoroscopically guided procedures. Rockville, MD: Center for De-

vices and Radiological Health, FDA, 1994.
5. Wagner LK. Biological effects of high x-ray doses. In: Balter, S Shope T, eds. Syllabus: a categorical course in physics. Oak Brook, IL: Radiological Society of North America, 1995;167–170.
6. International Commission on Radiological Protection. Avoidance of radiation injuries from medical interventional procedures. Annals of the ICRP. ICRP Publication 85. Oxford, UK: Pergamon Press, 2000. Issue 2.
7. International Commission on Radiological Protection. Diagnostic reference levels in medical imaging: review and additional advice. Annals of the ICRP. ICRP Supporting Guidance 2. Oxford, UK: Pergamon Press, 2001:33–52.
8. European Union. On Health Protection of Individuals against the Dangers of Ionizing Radiation to Medical Exposure, Council Directive 97/43/Euratom. Official J Eur Comm 1997; 180:22–27.
9. European Commission. Guidance on Diagnostic Reference Levels for Medical Exposures. Radiation Protection 1999;109.
10. Vano E, Gonzalez L. Approaches to establishing reference levels in interventional radiology. Radiat Prot Dosimetry 2001; 94:109–112.
11. Perisinakis K, Damilakis J, Theocharopoulos N, et al. Accurate assessment of patient effective radiation dose and associated detriment risk from radiofrequency catheter ablation procedures. Circulation 2001; 104:58–62.
12. McParland BJ. Entrance skin dose estimates derived from dose-area product measurements in interventional radiological procedures. Br J Radiol 1998; 71:1288–1295.
13. Williams JR. The interdependence of staff and patient doses in interventional radiology. Br J Radiol 1997; 70: 498–503.
14. Vano E, Gonzalez L, Fernadez JM, et al. Patient dose values in interventional radiology. Br J Radiol 1995; 68:1215–1220.
15. McParland BJ. A study of patient radiation doses in interventional radiological procedures. Br J Radiol 1998; 71:175–18.
16. Gkanatsios NA, Huda W, Peters KR. Adult patient doses in interventional procedures. Med Phys 2002; 29:717–723.
17. Schmidt PWE, Dance DR, Skinner CL, et al. Conversion factors of effective dose in pediatric cardiac angiography. Phys Med Biol 2000; 45:3095–3107.
18. Struelens L, Vanhavere F, Bosmans H, et al. Effective dose in angiography and interventional radiology: calculation of conversion coefficient for angiography of the lower limbs. Br J Radiol 2005; 78:135–142.
19. Briesmeister J, ed. MCNP—A General Monte Carlo N-particle transport code, version 4C2. Los Alamos National Laboratory Report, 2000:LA-13709-M.
20. Nowotny R, Hofer A. A program for calculating diagnostic x-ray spectra. Rofo 1985; 142:685–689.
21. International Commission on Radiological Protection. Recommendations of the International Commission on Radiological Protection. Annals of the ICRP. ICRP Publication 60. Oxford, UK: Pergamon Press, 1990; 21. Issue 1.
22. Eckerman K, Cristy M, Ryman J. The ORNL mathematical phantom series. 1986 Oak Ridge National Laboratory (ORNL) Report [Web site]. Available at: http://homer.hsr.ornl.gov/VLab/VLabPhan.html. Accessed May 1, 2005.
23. International Commission on Radiological Protection. Basic anatomical and physiological data for use in radiological protection: reference values. The International Commission on Radiological Protection, Report of the Task Group on Reference Man, 2002. ICRP Publication 89.
24. Perisinakis K, Theocharopoulos N, Karkavitsas N, et al. Patient effective radiation dose and associated risk from transmission scans using Gd-153 line sources in cardiac SPECT studies. Health Phys 2002; 83: 66–74.
25. National Research Council. Health effects exposure to low levels of ionizing radiation, BEIR V. Washington, DC: National Academy Press, 1990.
26. Cruces RR, Garcia-Granados J, Diaz Romero FJ, et al. Estimation of effective dose in some angiographic and interventional procedures. Br J Radiol 1998; 71:42–47.
27. Hart D, Jones G, Wall BF. Estimation of effective dose in diagnostic radiology from entrance surface dose and dose-area product measurements. NRPB-R262. Chilton, UK: NRPB, 1994; 1–57.
28. Hidajat N, Maurer J, Schroder RJ, et al. Radiation exposure in spiral computed tomography: dose distribution and dose reduction. Invest Radiol 1999; 34: 51–57.
29. Mueller PR, vanSonnenberg E, Ferrucci JT Jr. Percutaneous biliary drainage: technical and catheter-related problems in 200 procedures. AJR Am J Roentgenol 1982; 138:17–23.